AGU ADVANCING EARTH AND SPACE SCIENCES

Geophysical Research Letters

RESEARCH LETTER
10.1029/2023GL107567

Polar Vortex Disruptions by High Latitude Ocean Warming

Mostafa E. Hamouda[1,2,3], Alice Portal[4], and Claudia Pasquero[5]

[1]Institute for Atmosphere and Environment, Goethe University Frankfurt, Frankfurt am Main, Germany, [2]Astronomy and Meteorology Department, Faculty of Science, Cairo University, Cairo, Egypt, [3]Department of Civil and Environmental Engineering, Massachusetts Institute of Techonology, Cambridge, MA, USA, [4]Institute of Geography, Oeschger Centre for Climate Change Research, University of Bern, Bern, Switzerland, [5]Department of Earth and Environmental Sciences, University of Milan-Bicocca, Milan, Italy

Key Points:

- Around 65% of weak polar vortex (WPV) events are preceded by tropospheric pressure anomalies
- High-latitude ocean warming explains tropospheric air mass modification, which favors upward wave flux that disrupts the stratosphere
- Probabilistic forecast of WPV events is possible using an index of high-latitude ocean warming

Supporting Information:

Supporting Information may be found in the online version of this article.

Correspondence to:

M. E. Hamouda,
mhamouda@mit.edu

Citation:

Hamouda, M. E., Portal, A., & Pasquero, C. (2024). Polar vortex disruptions by high latitude ocean warming. *Geophysical Research Letters*, *51*, e2023GL107567. https://doi.org/10.1029/2023GL107567

Received 6 DEC 2023
Accepted 31 MAR 2024

Author Contributions:

Conceptualization: Mostafa E. Hamouda, Claudia Pasquero
Formal analysis: Mostafa E. Hamouda, Alice Portal
Investigation: Mostafa E. Hamouda, Alice Portal, Claudia Pasquero
Methodology: Mostafa E. Hamouda, Alice Portal, Claudia Pasquero
Resources: Mostafa E. Hamouda
Supervision: Claudia Pasquero
Validation: Mostafa E. Hamouda
Visualization: Mostafa E. Hamouda
Writing – original draft: Mostafa E. Hamouda, Claudia Pasquero
Writing – review & editing: Mostafa E. Hamouda, Alice Portal, Claudia Pasquero

Abstract

Mid-latitude extreme cold outbreaks are associated with disruptions of the polar vortex, which often happen abruptly in connection to a sudden stratospheric warming. Understanding global warming (particularly Arctic amplification) impacts on forecasting such events is challenging for the scientific community. Here we apply clustering analysis on the Northern Annular Mode to identify surface precursors and the governing mechanisms causing polar vortex disruption events. Two clusters of vortex breakdown emerge; 65% of the events, mainly displacements, are associated with high-latitude Ocean warming in the North Pacific and in Barents-Kara Sea. Such warming may cause large scale modifications of the tropospheric flow that favors a slowdown of the stratospheric vortex. The persistence of Ocean surface temperature patterns favors polar vortex disruptions, potentially improving prediction skills at the sub-seasonal to seasonal time scales.

Plain Language Summary

Extreme winter weather is linked to cold arctic outbreaks when the polar air mass spills frigid air to mid-latitudes. This phenomenon often follows weak polar vortex (in extreme cases a Sudden Stratospheric Warming) episodes. Forecasting such events is challenging as many climatic components can be involved. In this study, it is found that 65% of the events start with a certain surface air mass distribution (Low Pressure over the North Pacific, High Pressure over Eurasia). Such distribution is triggered by high latitude ocean warming corresponding to warm temperature anomalies in the North Pacific Ocean and Sea Ice loss in Barents-Kara seas. This result helps predicting the probability of polar vortex disruptions in winter, potentially leading to enhanced sub-seasonal to seasonal cold outbreaks forecast.

1. Introduction

In winter, the Stratospheric Polar Vortex (SPV) draws the attention of experts and non-experts, considering its severe impact on surface weather 2–4 weeks after SPV weakening (Baldwin et al., 2021).

The strength of the SPV is often measured using the Northern Annular Mode (NAM) index computed in the stratosphere at the 10 hPa pressure level (Baldwin & Dunkerton, 1999). When referring to surface conditions the NAM is known as Arctic Oscillation (AO), and corresponds to a hemispheric scale pattern of climate variability associated with meridional shifts of air masses between high and mid-latitudes. Meridional air mass displacements couple with the jet stream (Thompson & Wallace, 1998), so that a strong and steady tropospheric jet confines frigid Arctic air over the North Pole (positive AO phase), while a meandering jet spills cold polar air to the mid-latitudes in exchange of southern warm air (negative AO phase).

Baldwin and Dunkerton (2001) revealed a downward influence of the SPV on the troposphere: a strong SPV fosters a positive surface AO, associated with a steady and poleward displaced jet stream; a weak polar vortex (WPV) or in extreme cases a Sudden Stratospheric Warming (SSW) event (Charlton & Polvani, 2007), corresponds to a slowdown or a reversal of the zonal winds in the stratosphere, and favors negative AO and a meandering jet stream. Such conditions can lead to large thermal anomalies in the lower troposphere and extreme weather at the surface (Cohen et al., 2014, 2021; King et al., 2019; Xu et al., 2022).

The research community strives for sources of mid-latitude weather predictability to foresee WPV/SSW events ahead of time, motivated by the direct effects on sub-seasonal to seasonal mid-latitude weather predictions (Kidston et al., 2015). Various possible precursors have been identified in the literature. The occurrence of WPV events is often related to preceding tropospheric conditions both in the tropics and in the extratropics. In the tropical region, studies evidenced links with the phase of the El Niño/Southern Oscillation (Butler &

Polvani, 2011; Domeisen et al., 2019), of the Madden-Julian Oscillation (Kang & Tziperman, 2017, 2018), and of the Quasi-Biennial Oscillation (Baldwin et al., 2001; Elsbury et al., 2021). In mid-latitudes, North Pacific Sea Surface Temperature (SST) anomalies (Ayarzagüena et al., 2021; Hurwitz et al., 2012), as well as blocking events and bomb cyclones have been identified as possible precursors (Attard & Lang, 2019; Peings, 2019). In high latitudes, links with snow cover and sea ice in the Arctic region have been found (Cohen et al., 2007; Delhaye et al., 2023; Furtado et al., 2016; Ruggieri et al., 2017; Zhang et al., 2022). In other cases, no traceable tropospheric source was identified (Birner & Albers, 2017), indicating that some SSW events are simply triggered by favorable stratospheric internal variability (Scott & Polvani, 2004). The existence of such a variety of scenarios conducive to a strong weakening of the polar vortex has limited the development of statistical WPV predictions.

In this study, a new perspective for the identification of surface precursors of SSW events is introduced and applied to reanalysis data. A clustering of WPV events based on the atmospheric conditions in the previous 2 weeks shows that over 65% of the events have a clear surface signal before developing in the stratosphere. We show that a combination of the surface precursors emerging from this approach favors the occurrence of WPV. Moreover, the importance of high-latitude ocean warming is highlighted, whereas we argue that lower-latitude anomalies can cause modifications that are only limited to the tropospheric flow.

2. Data and Methods

2.1. Data

Geopotential height (GPH), wind, and air temperature between 1,000 and 10 hPa for 1979–2021 are obtained from the NCEP Climate Forecast System Reanalysis (CFSR, CFSv2) (Saha et al., 2010, 2014), and ERA5 reanalysis (Hersbach et al., 2020) from the European Center for Medium-Range Weather Forecasts. Model data are obtained from the Coupled Model Intercomparison Project (CMIP5) using MPI-ESM-LR 1950–2000 (Marsland et al., 2003) and IPSL-CM5A-LR 1901–2000 (Dufresne et al., 2013).

SST and sea ice concentration (SIC) data are obtained from the Met Office Hadley Centre (Rayner et al., 2003), with a monthly temporal resolution and a horizontal resolution of $1^\circ \times 1^\circ$.

2.2. Hierarchical Clustering and Composites

To group similar weak stratospheric polar events based on their time-height development of the NAM index (defined in Text S1.1 in Supporting Information S1), hierarchical clustering is employed as follows. For each weak vortex event (defined by 10 hPa NAM <-1.5), the NAM index between -15 and 0 days for all pressure levels (magenta lines in Figure 1a) is recorded in a matrix. Distance between events is defined as the Euclidean distance between the two matrices. A hierarchy of clusters is generated by merging one pair of nearest events or cluster of events at each step (Wilks, 2011). Clustering is stopped when the total intra-cluster distance becomes nearly constant after increasing the number of clusters (elbow method similar to Kretschmer et al. (2018)).

The composite of Decoupled events (Figure 4) is obtained by selecting the events in which a negative NAM index is observed on the surface during a strong stratospheric vortex (1,000 hPa average NAM <-1 within 10 days centered at day 0, and 10 hPa NAM >0.5), ensuring that the negative surface NAM is not a residual from a previous WPV, and requiring that the stratospheric vortex remains above zero (10 hPa NAM >0 over the following month).

3. Results and Discussion

3.1. Weak Polar Vortex Clusters and Precursors

The classical stratosphere-troposphere coupling, as first introduced by Baldwin and Dunkerton (1999, 2001), is illustrated in Figure 1a. Using the NAM index, which describes the strength of the SPV, the “dripping paint” pattern shows that the onset of WPV events (time 0) is followed, within 2–4 weeks on average, by changes in surface weather conditions.

Different classification criteria are employed in the literature to differentiate among WPV events based, for instance, on the morphology or on the strength of the anomalies (Baldwin et al., 2021). Hierarchical clustering has also been applied to identify spatially different SPV states (Kretschmer et al., 2018). Here a new approach is developed by basing the hierarchical clustering on the evolution of the NAM index through the atmospheric

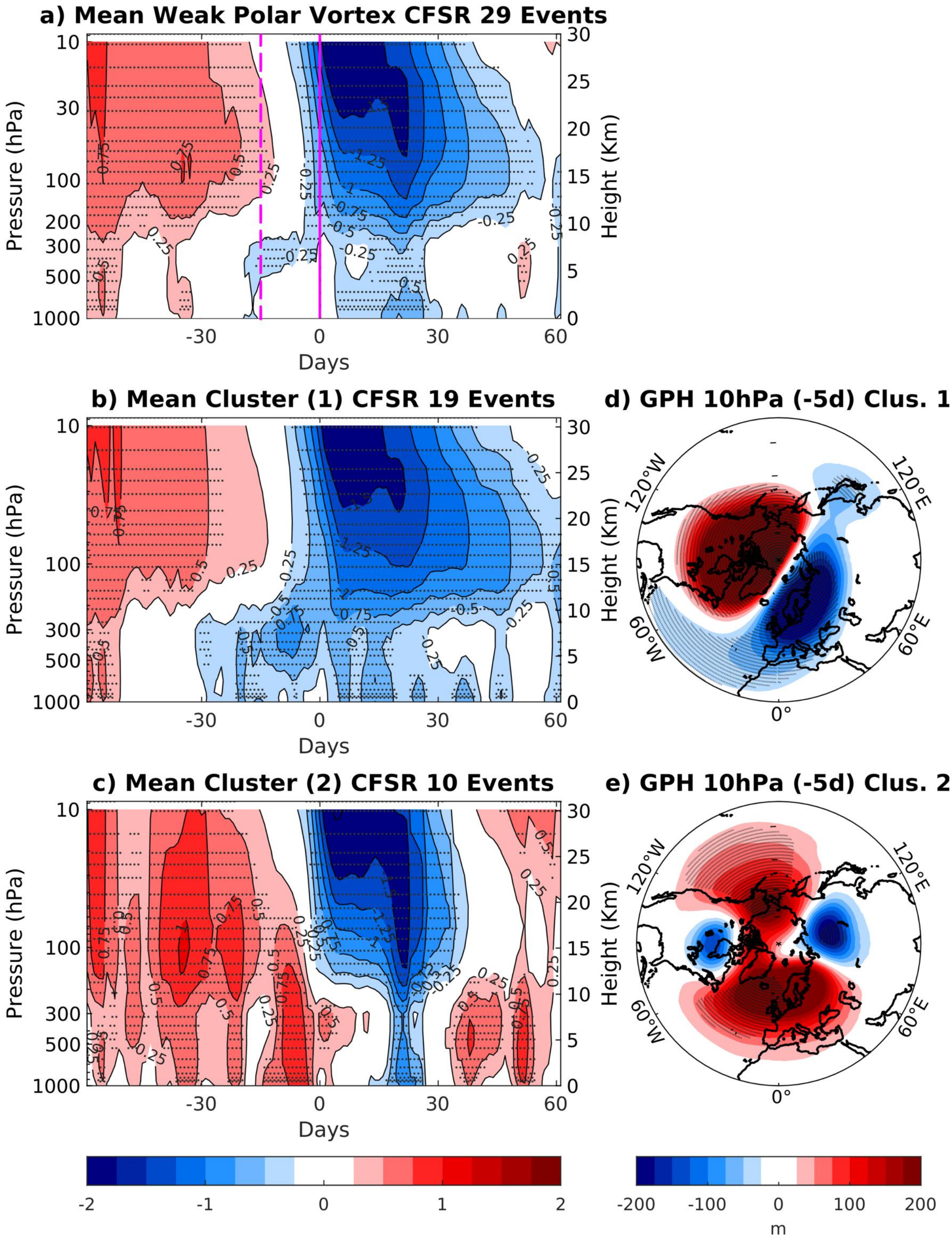

Figure 1. Composite of weak polar vortex (WPV) events using Northern Annular Mode index in the period 1979–2022. The onset of WPV is at day 0, and negative and positive days refer to periods of time before and after the onset respectively. Negative (positive) values are associated with weak (strong) stratospheric polar vortex and negative (positive) Arctic Oscillation phase at the surface. (a) Composite of all events (29), (b and c) Composite of events in cluster 1 (19 events) and 2 (10 events) separately. Downward coupling is evident in all panels; upward propagation is noticeable in cluster 1. Magenta box in panel (a) indicates the space-time span over which the clustering technique is applied. Geopotential height anomalies (unit m) at 10 hPa 5 days before the onset are composited for (d) Cluster 1; vortex displacement, (e) Cluster 2; vortex splits. Stippling shows significant anomalies at the 90th percentile significance level by bootstrapping for (a–c) and using two-sided Student's *t*-test for (d and e).

column within the 15 days preceding the onset of WPV conditions. This aims to differentiate the events which have a preceding tropospheric signal, from those that do not. The 29 events in the data set of NCEP reanalysis from 1979 to 2022 are grouped in two clusters (similar analysis for ERA5 reanalysis in sup. Figure 1). In the larger cluster (Cluster 1 hereafter, 19 events) a persistent negative AO signal appears in the troposphere about 3 weeks before the WPV (Figure 1b). Cluster 2 instead groups events with a positive AO phase before the onset of the WPV event (Figure 1c). Events dates are in Tables S2 and S3 in Supporting Information S1.

Beside the different time-height evolution of the tropospheric NAM in both clusters, the WPV has different morphologies: the average of cluster 1 events is characterized by polar vortex displacement off the pole, while cluster 2 composite corresponds to a polar vortex split into two smaller vortices (Figures 1d and 1e). Clustering on the time-height development of the NAM index yields consistent features compared to Charlton and Polvani (2007), Cohen and Jones (2011), and Karpechko et al. (2017), whose approach to tropospheric precursors starts from the classification of SSWs by morphology (i.e., splits and displacements), therefore evidencing the different nature and evolution of the two types of SPV weakening (Mitchell et al., 2013). In both cases, after the SPV weakening, a downward stratosphere-troposphere coupling may establish, resulting in a negative AO signal at the surface.

In the following we focus on the origin of the tropospheric NAM signal anticipating the occurrence of cluster-1 WPV events (Cluster 2 conditions are shown Figure S2 in Supporting Information S1).

The tropospheric conditions preceding the onset of the WPV events for cluster 1 are illustrated in Figure 2, which displays average anomalies with respect to the seasonal cycle of: 1,000 hPa GPH and 200 hPa vertical Wave Activity Flux (WAFz) (averaged 15–10 days before WPV onset). SST and SIC are anomalies of the month in which the event occurred, since ocean variability has a long time scale.

Upward dynamical coupling between troposphere and stratosphere occurs through the vertical propagation of planetary waves, which induces modifications in the stratospheric circulation (i.e., relative vorticity anomalies generated by anomalous cooling/warming of the stratosphere). Only large-scale forcing (typically wave 1 and 2), that are climatologically associated with longitudinal land-sea thermal contrasts and orographic forcing (Held & Ting, 1990; Lindgren et al., 2018; Portal et al., 2022), may propagate upward to affect the strong winter stratospheric mean flow (Andrews et al., 1987). Such waves break in the mid-stratosphere due to non-linear wave–mean flow interaction (Sjoberg & Birner, 2014), slowing down the polar vortex and transporting heat to the polar stratosphere.

The combination of the anomalous trough over the Aleutian Low in the North Pacific and the anomalous ridge over Eurasia (wave-1 anomalies; Figure 2a) compose a pattern that explains the overall surface negative NAM index (high latitude positive and mid-latitude negative anomalies in GPH), and that anticipates the negative NAM in the stratosphere (Köhler et al., 2023). This pattern is not to be confused with the negative NAM that emerges after the stratosphere-troposphere coupling (Figure S3 in Supporting Information S1), which is typically more zonally symmetric (Charlton-Perez et al., 2018).

At the surface and through the troposphere, the anomalous wave-1 GPH anomalies preceding the WPV interfere constructively with the climatological waves, resulting in an amplification of the large scale stationary waves (cf., Figure S4a in Supporting Information S1 with climatological wave-1 contours in Figure 8a of Hu et al. (2019)). By WAFz definition, this results in a large tropopause wave forcing (Figure 2d and Figure S4a in Supporting Information S1) and in a warming of the polar stratosphere (Cohen & Jones, 2011; Cohen et al., 2007; Matsuno, 1971). Such a GPH pattern is recurrent in the Northern Hemisphere (Kushnir & Wallace, 1989), however the persistence of this pattern is required to provide sufficient wave forcing to disrupt the stratospheric flow (Harnik, 2009). Our analysis suggests that such persistence can be provided by the presence of enduring oceanic surface anomalies, particularly in the North Pacific SST and in the Barents-Kara sea ice concentration (BK-SIC) (Figures 2b and 2c). Over the North Pacific, cluster 1 composite shows anomalous SST with warm anomalies near the Aleutian islands and cold anomalies around 45°N, in a pattern that projects onto the Pacific Decadal Oscillation (PDO) (Figure 2b).

The high-latitude North Pacific warm SST favors the development/deepening of the Aleutian low pressure (Figure 2a) (Ting, 1991). This is consistent with the modulation of SSW frequency related to the phase of the PDO on the decadal and sub-decadal time scales (Ayarzagüena et al., 2021; Hu & Guan, 2018; Woo et al., 2015).

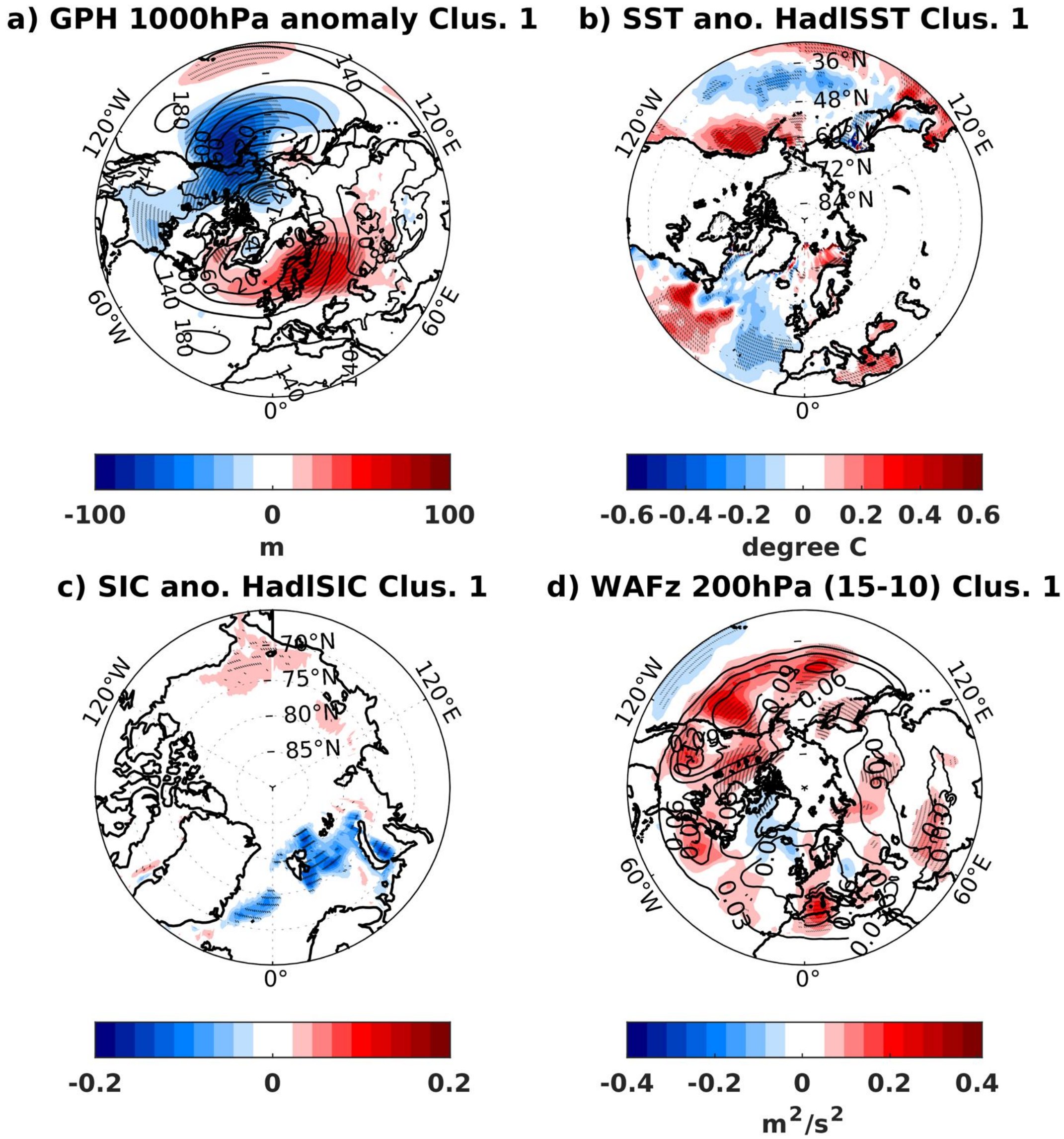

Figure 2. Troposphere conditions leading Cluster 1 weak polar vortex (WPV) events. (a) Geopotential height anomalies at 1,000 hPa 15–10 days before the onset of a WPV event in m (b) Sea surface temperature anomalies (HadlSST) in the month of the onset of WPV event in °C. (c) Sea ice concentration anomalies (HadlSIC) in the month of the onset of WPV event in %. (d) Wave-activity flux anomalies in the vertical direction at 200 hPa level averaged 15–10 days before the onset of a WPV event in $m^2\ s^{-2}$. Solid lines show climatological values. Stippling shows significant anomalies at the 90th percentile significance level using two-sided Student's *t*-test.

Moreover, the significant loss of BK-SIC emerging in cluster 1 (Figure 2c) is known to anticipate WPV events by enhancing wave propagation toward the stratosphere (Kim et al., 2014; Ruggieri et al., 2017; Sun et al., 2015).

To highlight the atmospheric response to SST and SIC anomalies, two monthly time series are obtained from November to February anomalies of North Pacific SST and BK-SIC separately (Figure S5 in Supporting Information S1, for the regions over which the anomalies are computed). 1,000 hPa GPH anomaly is regressed onto two new time series (Text S1.3 in Supporting Information S1), the first is based on North Pacific SST anomalies (index = A–B and regression Figures S6a and S6b in Supporting Information S1), the second is by combining North Pacific SST with BK-SIC anomalies (index = A–B–C and regression in Figures 3a and 3b). The results show the association of a deeper Aleutian Low with warmer North Pacific SST, and anomalously high pressure over the Arctic. The loss of SIC results in ridging over Eurasia and the Ural region (not shown). A combination of

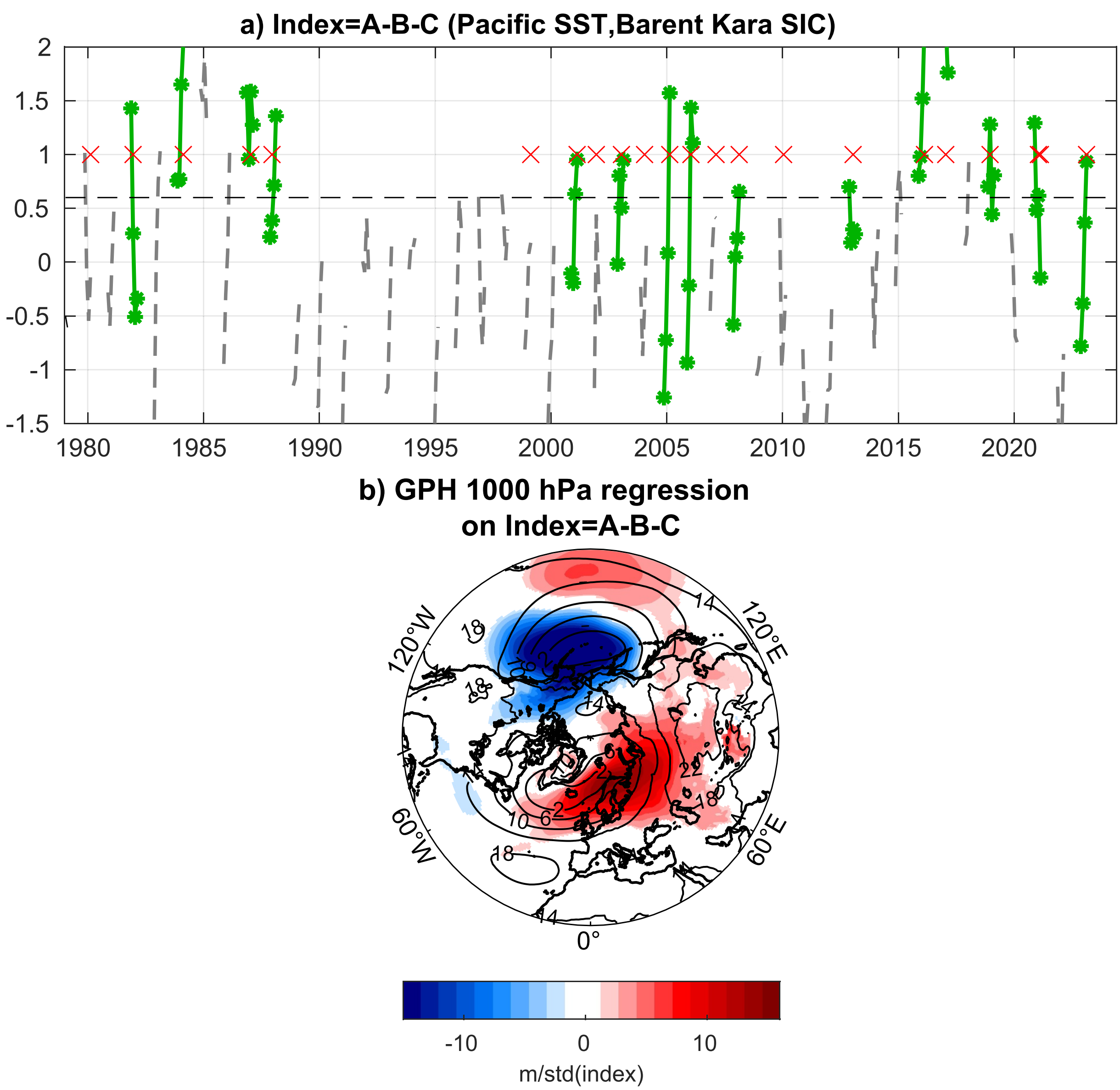

Figure 3. Atmospheric response associated with ocean warming. (a) Time series of the calculated index based on the boxes Figure S6 in Supporting Information S1. Pacific sea surface temperature anomalies (A and B for the warm and the cold regions respectively) and Barents-Kara sea ice loss (C): Index = A–B–C. The correct predictions (hits) of cluster-1 type weak polar vortex are shown in green lines. Index crossing 0.6 threshold is considered. (b) Regression of geopotential height (GPH) at 1,000 hPa onto index A–B–C in panel (a). Unit: Meter per standard deviation of index. Anomalies with less than 90% significance level are omitted using *t*-test. Contour lines show 1,000 hPa GPH climatology in meters/10. Pattern correlation of panel (b) with Figure 2a equals 0.84.

both surface conditions yields a pattern (Figure 3b and Figure S8 in Supporting Information S1) which is favorable for WPV as in Figure 2a and Figure S2a in Supporting Information S1.

The main limitation to this analysis is the small sample of events (19 events), which limits the generalization of the conclusions regarding the association with surface conditions. Therefore, a similar analysis is applied further on two models, IPSL-CM5A-LR and MPI-ESM-LR, which evidence proper stratospheric variability (Charlton-Perez et al., 2013), and were studied in the context of stratosphere-troposphere coupling (Hamouda et al., 2021). The results, based on the historical period (Figure S7 in Supporting Information S1), show a similar North Pacific SST pattern associated with cluster-1 type events in both models, giving more confidence to the conclusions based on reanalysis.

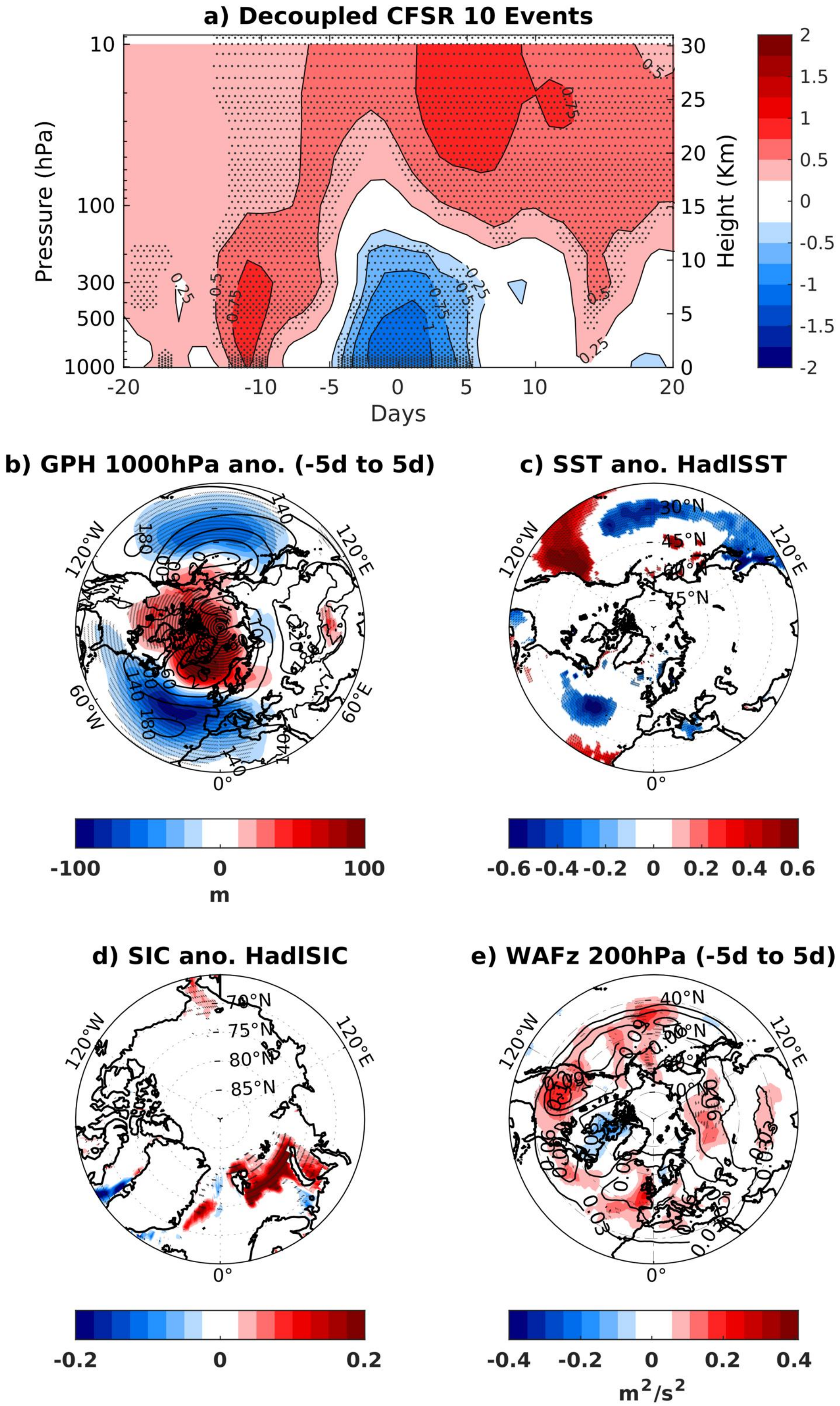
a) Decoupled CFSR 10 Events
Pressure (hPa)
Height (Km)
Days
b) GPH 1000hPa ano. (-5d to 5d)
m
c) SST ano. HadISST
d) SIC ano. HadISIC
e) WAFz 200hPa (-5d to 5d)
m²/s²

Figure 4.

The peculiarity of the surface conditions in cluster 1 (North Pacific SST and BK-SIC) can be used to predict the occurrence WPV events. With this aim, we use the monthly indices based on their anomalies (computed over the boxes Figure S5 in Supporting Information S1 and described in Text S1.3 in Supporting Information S1). Most cluster 1 events are associated with favorable Pacific SST conditions (15 out of 21, Figure S6a in Supporting Information S1). However, false alarms based on the SST index are frequent (9 in 44 winters), resulting in an overestimation of the number of WPVs, with a detrimental effect on the overall performance of the index (0.41 in terms of binary Heidke Skill Score (Mason, 2003)). A similar issue can also be observed when considering only PDO index (Woo et al., 2015). Here we highlight the enhanced skill of prediction by using a different index obtained by combining the Pacific SST signal with BK sea-ice loss, which again allows the prediction of 15 WPV events (Figure 3a), but most importantly lowers the number of false alarms (6 instead of nine when considering only Pacific SSTs). The binary Heidke Skill Score reaches in this case a value of 0.50, evidencing the positive performance of the index with respect to random chance. However, a longer reanalysis record is needed to test the significance of the improvement.

From this we conclude that, in presence of surface negative NAM, the index based on the combination of North Pacific and BK sea surface anomalies shows the tendency of the system to develop upper level GPH disturbances that may trigger WPV events. A caveat for the use of this index as a predictor of WPV is that the internal variability of the stratosphere modulates the vertical wave propagation through the tropopause (de la Cámara et al., 2017; Sjoberg & Birner, 2012), so that not all tropospheric conditions favorable to vortex deceleration are expected to result in the occurrence of a WPV event (Further discussion in the next section). This and the presence of tropospheric variability unrelated with the identified surface forcing, explain why the index may issue incorrect forecasts. Nevertheless, based on the high fraction of correct guesses, the index successfully combines surface precursors to vortex weakening and can be used as a guideline to forecast PV-displacement events (e.g., statistical predictions (Jucker & Reichler, 2018)).

3.2. Stratosphere-Troposphere Decoupling

In cluster 1, the negative phase of the NAM starts in the troposphere and propagates toward the stratosphere. However, not all negative tropospheric NAM conditions propagate into the stratosphere. The vertical propagation of tropospheric waves above the tropopause depends on the state of the SPV, which is more or less susceptible to wave breaking and deceleration depending on the strength and position of the mean flow (Birner & Albers, 2017; de la Cámara et al., 2017; Sjoberg & Birner, 2012).

To distinguish surface conditions that induce SPV weakening from those which do not, further analysis is carried out to include the cases in which a negative AO phase is trapped in the troposphere, decoupled from the stratosphere. To this end, a composite analysis is applied on surface negative NAM events that occur during a strong polar vortex signals, and do not propagate upward to induce a WPV in the stratosphere. The composite for such events is denominated Decoupled (further described in Methods) and is shown in Figure 4 (Table S4 in Supporting Information S1 for the dates).

In the Decoupled composite, shown in Figure 4a featuring opposite NAM anomalies in the stratosphere and troposphere, Figure 4c shows that cold Pacific and Atlantic SST anomalies weaken the SST meridional gradients north of 35°N (Figure 4c) and are associated with a slowdown of the mid-latitude tropospheric jetstream (Figure S9 in Supporting Information S1), which is consistent with negative AO and North Atlantic Oscillation conditions (Figure 4b). Positive SIC anomalies (Figure 4d) support a strong polar vortex as opposed to cluster-1 SIC negative anomalies. The Decoupled composite differs from cluster 1 in two aspects. One is that the absence of surface anomalies in high latitudes seems to confine the negative NAM anomalies to the troposphere, and is not associated with a significant deceleration of the stratospheric vortex (Chen & Trenberth, 1988). The other is that cluster 1 GPH anomaly is essentially a zonal wave-1 perturbation, which magnifies the stationary waves (by

Figure 4. Stratosphere-troposphere decoupling. (a) Composite of time-height Northern Annular Mode index showing the Decoupled events between the stratosphere and the troposphere. (b) Geopotential height anomalies at 1,000 hPa averaged −5–5 days in m. (c) Sea surface temperature anomalies in the month of the event in °C. (d) Sea ice concentration anomalies in the month of the event in %. (e) Wave-activity flux anomalies in the vertical direction at 200 hPa, averaged 15–10 days before the event in $m^2\ s^{-2}$. Solid lines show climatological values. Stippling shows significant anomalies at the 90th percentile significance level by bootstrapping for (a) and using two-sided Student's t-test for the rest.

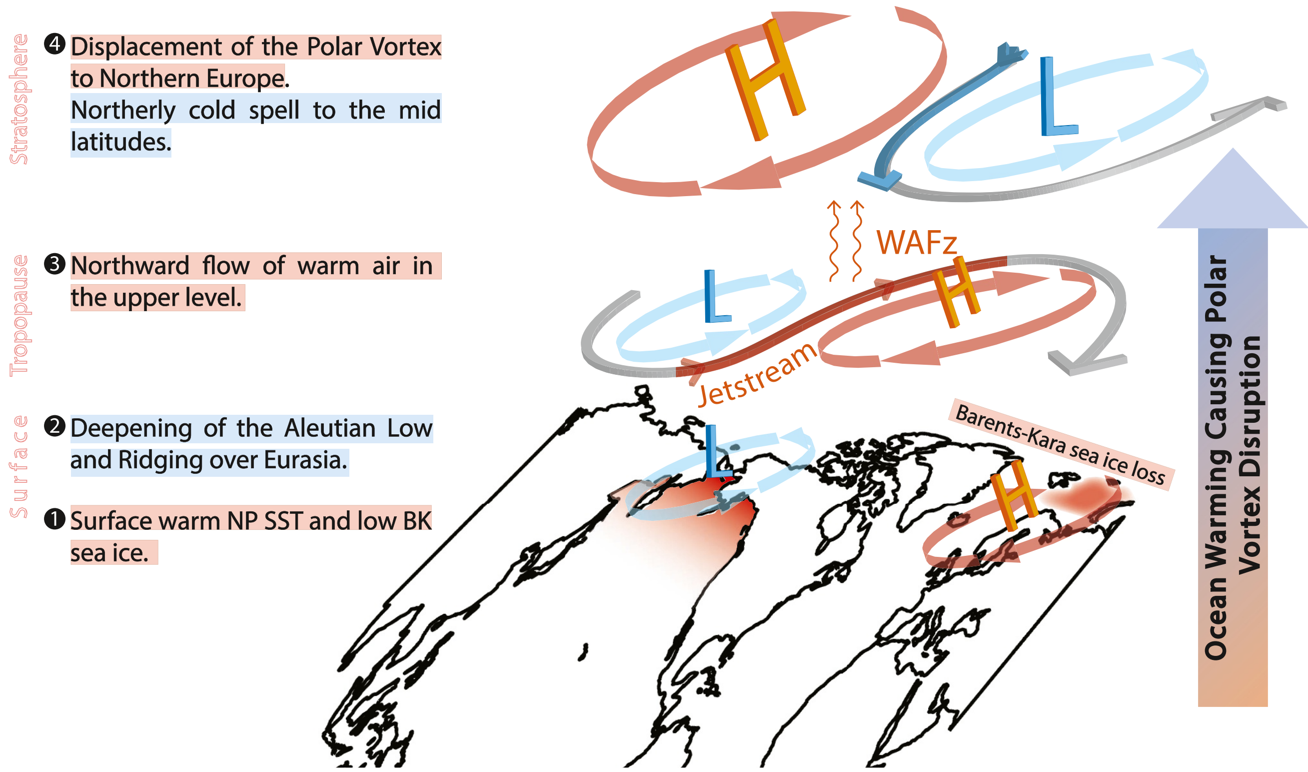

Figure 5. Schematic view of ocean warming influence on polar vortex displacement. (a and b) Warm sea surface temperature anomalies in the North Pacific deepen the Aleutian Low pressure, and Barents-Kara sea ice loss locally cause high pressure anomalies. (c) Corresponding anomalies in the upper troposphere cause Northward flow of warm mid-latitude air into the polar region. (d) Through upward wave forcing at the tropopause, warm southerly air is transported into the polar stratosphere causing a displacement of the polar vortex, resulting in an extremely cold return flow toward the mid-latitudes.

superposing to the dipole above Eurasia and North Pacific). In the Decoupled composite, the GPH anomaly is rather annular (zonally symmetric) and does not produce the upper level zonal gradients (not shown), resulting in weak WAFz anomalies as illustrated in Figure 4e.

4. Summary and Conclusion

Hierarchical clustering analysis on the tropospheric conditions preceding polar vortex breakdown shows that 65% of WPV events (displacements on average) are associated with high latitude ocean surface warming (temperature anomalies in the North Pacific and sea ice loss in BK seas). The mechanism by which these conditions perturb the stratosphere is sketched in Figure 5, and is summarized hereafter.

Ocean anomalies in the Aleutian region and in the BK (Hurwitz et al., 2012; Ruggieri et al., 2017) sea generate pressure perturbations of opposite signs over two high latitude regions which result in the amplification of the large scale tropospheric waves, mainly in the Pacific-American sector. The anomalies propagate vertically to the stratosphere, modifying the zonal flow in such a way that southerly air is transported into the polar stratosphere, favoring the displacement of the stratospheric vortex off the North Pole toward Eurasia. This mechanism, presented in Garfinkel et al. (2010) and applied for example, to explain the decadal variability of SSWs through phases of the PDO (Ayarzagüena et al., 2021), is exploited here to show the importance of high-latitude ocean warming in the stratosphere-troposphere coupling during displacement events, in contrast to the possible decoupling in the absence of high-latitude warming.

The results presented here can also be useful for sub-seasonal predictions. The classical downward propagating anomalies from the stratosphere into the troposphere improve the performance of 2–4 weeks weather forecasts (Butler et al., 2016; Domeisen et al., 2020). The identification of the conditions leading to cluster-1 type events has permitted the definition of an index that can be used as a precursor for SPV weakening and could thus increase the skill of weather predictions at and beyond the sub-seasonal time scale. To this purpose, the long memory of oceans can be employed in terms of SST and sea ice anomalies, since they can generate long lasting tropospheric perturbations necessary to trigger displacement events. Typically, high-frequency tropospheric wave activity may not be sufficient to perturb the stratosphere (Baldwin et al., 2021; Harnik, 2009; Sjoberg & Birner, 2012).

Further analysis (on the Decoupled composite) indicates that conditions displaying a similar zonal pressure anomaly (negative AO signal), though lacking the longitudinal and high-latitude surface signal, generate perturbations that do not affect the stratosphere. This supports further research on the possible effects of anthropogenic climate change on polar vortex breakouts, focusing on the local manifestation of the warming rather than on zonal or global mean signals.

In closing, it is worth highlighting that in long-term projections of a high emission scenario, cluster-1 type WPV, that is, with preceding upward troposphere-stratosphere NAM coupling, were shown to become dominant over cluster-2 WPV (Hamouda et al., 2021). The warming of the high latitude North Pacific was found to be a robust explanation for such a regime transition. The results presented here, showing a strong coupling of cluster-1 WPV with persistent sea-surface and tropospheric precursors, suggest a tendency toward enhanced predictability of WPV events in a warmer climate.

Data Availability Statement

NOAA-NCEP reanalysis and CMIP5 data sets are available on https://esgf-node.llnl.gov/search/esgf-llnl/ under reanalysis and CMIP5 projects. Search criteria for NOAA reanalysis are: CREATE-IP project and NCEP Institute; For IPSL and MPI: select CMIP5 project, then IPSL and MPI models. ERA5 is available at the Copernicus Climate Change Service Climate Data Store Hersbach et al. (2023). Hierarchical clustering is performed by python library https://docs.scipy.org/doc/scipy/reference/cluster.hierarchy.html.

Acknowledgments

M.E.H. is grateful for the support by the German Research Foundation (Deutsche Forschungsgemeinschaft, DFG) for the research group FOR 2416 "Space-Time Dynamics of Extreme Floods (SPATE)" (project number 278017089), and the acquisition by Bodo Ahrens is appreciated. The resources of the German Climate Computing Center (DKRZ) granted by its Scientific Steering Committee (WLA) under project ID bb1064 was used for the processing of some data. M.E.H. appreciates the efforts of Rabab Essam in designing the sketch of Figure 5. Open access funding enabled and organized by Projekt DEAL.

References

Andrews, D. G., Holton, J. R., & Leovy, C. B. (1987). *Middle atmosphere dynamics* (Vol. 40). Academic Press.

Attard, H. E., & Lang, A. L. (2019). Troposphere–stratosphere coupling following tropospheric blocking and extratropical cyclones. *Monthly Weather Review*, *147*(5), 1781–1804. https://doi.org/10.1175/MWR-D-18-0335.1

Ayarzagüena, B., Manzini, E., Calvo, N., & Matei, D. (2021). Interaction between decadal-to-multidecadal oceanic variability and sudden stratospheric warmings. *Annals of the New York Academy of Sciences*, *1504*(1), 215–229. https://doi.org/10.1111/nyas.14663

Baldwin, M. P., Ayarzagüena, B., Birner, T., Butchart, N., Butler, A. H., Charlton-Perez, A. J., et al. (2021). Sudden stratospheric warmings. *Reviews of Geophysics*, *59*(1). e2020RG000708. https://doi.org/10.1029/2020rg000708

Baldwin, M. P., & Dunkerton, T. (1999). Propagation of the Arctic Oscillation from the stratosphere to the troposphere. *Journal of Geophysical Research*, *104*(D24), 30937–30946.

Baldwin, M. P., & Dunkerton, T. (2001). Stratospheric harbingers of anomalous weather regimes. *Science*, *294*(5542), 581–584. https://doi.org/10.1126/science.1063315

Baldwin, M. P., Gray, L. J., Dunkerton, T. J., Hamilton, K., Haynes, P. H., Randel, W. J., et al. (2001). The quasi-biennial oscillation. *Reviews of Geophysics*, *39*(2), 179–229. https://doi.org/10.1029/1999RG000073

Birner, T., & Albers, J. R. (2017). Sudden stratospheric warmings and anomalous upward wave activity flux. *Inside Solaris*, *13*(Special_Edition), 8–12. https://doi.org/10.2151/sola.13a-002

Butler, A. H., Arribas, A., Athanassiadou, M., Baehr, J., Calvo, N., Charlton-Perez, A., et al. (2016). The climate-system historical forecast project: Do stratosphere-resolving models make better seasonal climate predictions in boreal winter? *Quarterly Journal of the Royal Meteorological Society*, *142*(696), 1413–1427. https://doi.org/10.1002/qj.2743

Butler, A. H., & Polvani, L. M. (2011). El Niño, La Niña, and stratospheric sudden warmings: A revaluation in light of the observational record. *Geophysical Research Letters*, *38*(13), L13807. https://doi.org/10.1029/2011GL048084

Charlton, A. J., & Polvani, L. M. (2007). A new look at stratospheric sudden warmings. Part I: Climatology and modeling benchmarks. *Journal of Climate*, *20*(3), 449–469. https://doi.org/10.1175/jcli3996.1

Charlton-Perez, A. J., Baldwin, M. P., Birner, T., Black, R. X., Butler, A. H., Calvo, N., et al. (2013). On the lack of stratospheric dynamical variability in low-top versions of the CMIP5 models. *Journal of Geophysical Research: Atmospheres*, *118*(6), 2494–2505. https://doi.org/10.1002/jgrd.50125

Charlton-Perez, A. J., Ferranti, L., & Lee, R. W. (2018). The influence of the stratospheric state on North Atlantic weather regimes. *Quarterly Journal of the Royal Meteorological Society*, *144*(713), 1140–1151. https://doi.org/10.1002/qj.3280

Chen, S.-C., & Trenberth, K. E. (1988). Forced planetary waves in the Northern Hemisphere winter: Wave-coupled orographic and thermal forcing. *Journal of the Atmospheric Sciences*, *45*(4), 682–704. https://doi.org/10.1175/1520-0469(1988)045<0682:fpwitn>2.0.co;2

Cohen, J., Agel, L., Barlow, M., Garfinkel, C. I., & White, I. (2021). Linking Arctic variability and change with extreme winter weather in the United States. *Science*, *373*(6559), 1116–1121. https://doi.org/10.1126/science.abi9167

Cohen, J., Barlow, M., Kushner, P., & Saito, K. (2007). Stratosphere-troposphere coupling and links with Eurasian land surface variability. *Journal of Climate*, *20*(21), 5335–5343. https://doi.org/10.1175/2007jcli1725.1

Cohen, J., & Jones, J. (2011). Tropospheric precursors and stratospheric warmings. *Journal of Climate*, *24*(24), 6562–6572. https://doi.org/10.1175/2011jcli4160.1

Cohen, J., Screen, J., Furtado, J., Barlow, M., Whittleston, D., Coumou, D., et al. (2014). Recent arctic amplification and extreme mid-latitude weather. *Nature Geoscience*, *7*(9), 627–637. https://doi.org/10.1038/ngeo2234 de la Cámara, A., Albers, J. R., Birner, T., Garcia, R. R., Hitchcock, P., Kinnison, D. E., & Smith, A. K. (2017). Sensitivity of sudden stratospheric warmings to previous stratospheric conditions. *Journal of the Atmospheric Sciences*, *74*(9), 2857–2877. https://doi.org/10.1175/jas-d-17-0136.1

Delhaye, S., Massonnet, F., Fichefet, T., Msadek, R., Terray, L., & Screen, J. (2023). Dominant role of early winter Barents-Kara sea ice extent anomalies in subsequent atmospheric circulation changes in CMIP6 models. *Climate Dynamics*, 1–24. https://doi.org/10.21203/rs.3.rs-2617079/v1

Domeisen, D. I., Butler, A. H., Charlton-Perez, A. J., Ayarzagüena, B., Baldwin, M. P., Dunn-Sigouin, E., et al. (2020). The role of the stratosphere in subseasonal to seasonal prediction: 2. Predictability arising from stratosphere-troposphere coupling. *Journal of Geophysical Research: Atmospheres*, *125*(2). e2019JD030923. https://doi.org/10.1029/2019jd030923

Domeisen, D. I., Garfinkel, C. I., & Butler, A. H. (2019). The teleconnection of El Niño Southern Oscillation to the stratosphere. *Reviews of Geophysics*, *57*(1), 5–47. https://doi.org/10.1029/2018rg000596

Dufresne, J.-L., Foujols, M.-A., Denvil, S. E. A., Caubel, A., Marti, O., Aumont, O., et al. (2013). Climate change projections using the IPSL-CM5 earth system model: From CMIP3 to CMIP5. *Climate Dynamics*, *40*(9), 2123–2165. https://doi.org/10.1007/s00382-012-1636-1

Elsbury, D., Peings, Y., & Magnusdottir, G. (2021). Variation in the Holton–Tan effect by longitude. *Quarterly Journal of the Royal Meteorological Society*, *147*(736), 1767–1787. https://doi.org/10.1002/qj.3993

Furtado, J. C., Cohen, J. L., & Tziperman, E. (2016). The combined influences of autumnal snow and sea ice on Northern Hemisphere winters. *Geophysical Research Letters*, *43*(7), 3478–3485. https://doi.org/10.1002/2016gl068108

Garfinkel, C. I., Hartmann, D. L., & Sassi, F. (2010). Tropospheric precursors of anomalous Northern Hemisphere stratospheric polar vortices. *Journal of Climate*, *23*(12), 3282–3299. https://doi.org/10.1175/2010jcli3010.1

Hamouda, M. E., Pasquero, C., & Tziperman, E. (2021). Decoupling of the Arctic Oscillation and North Atlantic Oscillation in a warmer climate. *Nature Climate Change*, *11*(2), 137–142. https://doi.org/10.1038/s41558-020-00966-8

Harnik, N. (2009). Observed stratospheric downward reflection and its relation to upward pulses of wave activity. *Journal of Geophysical Research*, *114*(D8), D08120. https://doi.org/10.1029/2008jd010493

Held, I. M., & Ting, M. (1990). Orographic versus thermal forcing of stationary waves: The importance of the mean low-level wind. *Journal of the Atmospheric Sciences*, *47*(4), 495–500. https://doi.org/10.1175/1520-0469(1990)047<0495:ovtfos>2.0.co;2

Hersbach, H., Bell, B., Berrisford, P., Biavati, G., Horányi, A., Muñoz Sabater, J., et al. (2023). ERA5 hourly data on pressure levels from 1940 to present [Dataset]. *Copernicus Climate Change Service (C3S) Climate Data Store (CDS)*, https://doi.org/10.24381/cds.bd0915c6

Hersbach, H., Bell, B., Berrisford, P., Hirahara, S., Horányi, A., Muñoz-Sabater, J., et al. (2020). The ERA5 global reanalysis. *Quarterly Journal of the Royal Meteorological Society*, *146*(730), 1999–2049. https://doi.org/10.1002/qj.3803

Hu, D., & Guan, Z. (2018). Decadal relationship between the stratospheric Arctic vortex and Pacific decadal oscillation. *Journal of Climate*, *31*(9), 3371–3386. https://doi.org/10.1175/jcli-d-17-0266.1

Hu, D., Guan, Z., Guo, Y., Lu, C., & Jin, D. (2019). Dynamical connection between the stratospheric Arctic vortex and sea surface temperatures in the North Atlantic. *Climate Dynamics*, *53*(11), 6979–6993. https://doi.org/10.1007/s00382-019-04971-2

Hurwitz, M. M., Newman, P. A., & Garfinkel, C. I. (2012). On the influence of North Pacific sea surface temperature on the Arctic winter climate. *Journal of Geophysical Research*, *117*(D19), D19110. https://doi.org/10.1029/2012JD017819

Jucker, M., & Reichler, T. (2018). Dynamical precursors for statistical prediction of stratospheric sudden warming events. *Geophysical Research Letters*, *45*(23), 13–124. https://doi.org/10.1029/2018gl080691

Kang, W., & Tziperman, E. (2017). More frequent sudden stratospheric warming events due to enhanced MJO forcing expected in a warmer climate. *Journal of Climate*, *30*(21), 8727–8743. https://doi.org/10.1175/jcli-d-17-0044.1

Kang, W., & Tziperman, E. (2018). The MJO-SSW teleconnection: Interaction between MJO-forced waves and the mid-latitude jet. *Geophysical Research Letters*, *45*(9), 4400–4409. https://doi.org/10.1029/2018GL077937

Karpechko, A. Y., Hitchcock, P., Peters, D. H. W., & Schneidereit, A. (2017). Predictability of downward propagation of major sudden stratospheric warmings. *Quarterly Journal of the Royal Meteorological Society*, *143*(704), 1459–1470. https://doi.org/10.1002/qj.3017

Kidston, J., Scaife, A., Hardiman, S., Mitchell, D., Butchart, N., Baldwin, M., & Gray, L. (2015). Stratospheric influence on tropospheric jet streams, storm tracks and surface weather. *Nature Geoscience*, *8*(6), 433–440. https://doi.org/10.1038/ngeo2424

Kim, B. M., Son, S.-W., Min, S.-K., Jeong, J.-H., Kim, S.-J., Zhang, X., et al. (2014). Weakening of the stratospheric polar vortex by Arctic sea-ice loss. *Nature Communications*, *5*(1), 4646. https://doi.org/10.1038/ncomms5646

King, A. D., Butler, A. H., Jucker, M., Earl, N. O., & Rudeva, I. (2019). Observed relationships between sudden stratospheric warmings and European climate extremes. *Journal of Geophysical Research: Atmospheres*, *124*(24), 13943–13961. https://doi.org/10.1029/2019jd030480

Köhler, R. H., Jaiser, R., & Handorf, D. (2023). How do different pathways connect the stratospheric polar vortex to its tropospheric precursors? *Weather and Climate Dynamics*, *4*(4), 1071–1086. https://doi.org/10.5194/wcd-4-1071-2023

Kretschmer, M., Coumou, D., Agel, L., Barlow, M., Tziperman, E., & Cohen, J. (2018). More-persistent weak stratospheric polar vortex states linked to cold extremes. *Bulletin of the American Meteorological Society*, *99*(1), 49–60. https://doi.org/10.1175/bams-d-16-0259.1

Kushnir, Y., & Wallace, J. M. (1989). Low-frequency variability in the Northern Hemisphere winter: Geographical distribution, structure and time-scale dependence. *Journal of the Atmospheric Sciences*, *46*(20), 3122–3143. https://doi.org/10.1175/1520-0469(1989)046<3122:lfvitn>2.0.co;2

Lindgren, E., Sheshadri, A., & Plumb, R. (2018). Sudden stratospheric warming formation in an idealized general circulation model using three types of tropospheric forcing. *Journal of Geophysical Research: Atmospheres*, *123*(18), 10–125. https://doi.org/10.1029/2018jd028537

Marsland, S., Haak, H., Jungclaus, J., Latif, M., & Röske, F. (2003). The Max-Planck-Institute global ocean/sea ice model with orthogonal curvilinear coordinates. *Ocean Modelling*, *5*(2), 91–127. https://doi.org/10.1016/S1463-5003(02)00015-X

Mason, I. B. (2003). Binary events. In I. T. Jolliffe & D. B. Stephenson (Eds.), *Forecast verification: A practitioner's guide in atmospheric science*. Wiley.

Matsuno, T. (1971). A dynamical model of the stratospheric sudden warming. *Journal of the Atmospheric Sciences*, *28*(8), 1479–1494. https://doi.org/10.1175/1520-0469(1971)028<1479:admots>2.0.co;2

Mitchell, D. M., Gray, L. J., Anstey, J., Baldwin, M. P., & Charlton-Perez, A. J. (2013). The influence of stratospheric vortex displacements and splits on surface climate. *Journal of Climate*, *26*(8), 2668–2682. https://doi.org/10.1175/jcli-d-12-00030.1

Peings, Y. (2019). Ural blocking as a driver of early-winter stratospheric warmings. *Geophysical Research Letters*, *46*(10), 5460–5468. https://doi.org/10.1029/2019gl082097

Portal, A., Pasquero, C., D'Andrea, F., Davini, P., Hamouda, M. E., & Rivière, G. (2022). Influence of reduced winter land-sea contrast on the mid-latitude atmospheric circulation. *Journal of Climate*, *35*(19), 6237–6251. https://doi.org/10.1175/jcli-d-21-0941.1

Rayner, N. A., Parker, D. E., Horton, E. B., Folland, C. K., Alexander, L. V., Rowell, D. P., et al. (2003). Global analyses of sea surface temperature, sea ice, and night marine air temperature since the late nineteenth century. *Journal of Geophysical Research*, *108*(D14), 4407. https://doi.org/10.1029/2002jd002670

Ruggieri, P., Kucharski, F., Buizza, R., & Ambaum, M. H. P. (2017). The transient atmospheric response to a reduction of sea-ice cover in the Barents and Kara Seas. *Quarterly Journal of the Royal Meteorological Society*, *143*(704), 1632–1640. https://doi.org/10.1002/qj.3034

Saha, S., Moorthi, S., Pan, H.-L., Wu, X., Wang, J., Nadiga, S., et al. (2010). The NCEP climate forecast system reanalysis. *Bulletin of the American Meteorological Society*, *91*(8), 1015–1058. https://doi.org/10.1175/2010BAMS3001.1

Saha, S., Moorthi, S., Wu, X., Wang, J., Nadiga, S., Tripp, P., et al. (2014). The NCEP climate forecast system version 2. *Journal of Climate*, *27*(6), 2185–2208. https://doi.org/10.1175/jcli-d-12-00823.1

Scott, R., & Polvani, L. M. (2004). Stratospheric control of upward wave flux near the tropopause. *Geophysical Research Letters*, *31*(2), L02115. https://doi.org/10.1029/2003gl017965

Sjoberg, J. P., & Birner, T. (2012). Transient tropospheric forcing of sudden stratospheric warmings. *Journal of the Atmospheric Sciences*, *69*(11), 3420–3432. https://doi.org/10.1175/jas-d-11-0195.1

Sjoberg, J. P., & Birner, T. (2014). Stratospheric wave–mean flow feedbacks and sudden stratospheric warmings in a simple model forced by upward wave activity flux. *Journal of the Atmospheric Sciences*, *71*(11), 4055–4071. https://doi.org/10.1175/jas-d-14-0113.1

Sun, L., Deser, C., & Tomas, R. A. (2015). Mechanisms of stratospheric and tropospheric circulation response to projected Arctic sea ice loss. *Journal of Climate*, *28*(19), 7824–7845. https://doi.org/10.1175/jcli-d-15-0169.1

Thompson, D. W. J., & Wallace, J. M. (1998). The Arctic Oscillation signature in the wintertime geopotential height and temperature fields. *Geophysical Research Letters*, *25*(9), 1297–1300. https://doi.org/10.1029/98GL00950

Ting, M. (1991). The stationary wave response to a midlatitude SST anomaly in an idealized GCM. *Journal of the Atmospheric Sciences*, *48*(10), 1249–1275. https://doi.org/10.1175/1520-0469(1991)048<1249:tswrta>2.0.co;2

Wilks, D. S. (2011). *Statistical methods in the atmospheric sciences* (Vol. 100). Academic Press.

Woo, S.-H., Sung, M.-K., Son, S.-W., & Kug, J.-S. (2015). Connection between weak stratospheric vortex events and the Pacific Decadal Oscillation. *Climate Dynamics*, *45*(11–12), 3481–3492. https://doi.org/10.1007/s00382-015-2551-z

Xu, Q., Chen, W., & Song, L. (2022). Two leading modes in the evolution of major sudden stratospheric warmings and their distinctive surface influence. *Geophysical Research Letters*, *49*(2), e2021GL095431. https://doi.org/10.1029/2021GL095431

Zhang, J., Orsolini, Y., Limpasuvan, V., & Ukita, J. (2022). Impact of the Pacific sector sea ice loss on the sudden stratospheric warming characteristics. *npj Climate and Atmospheric Science*, *5*(1), 74. https://doi.org/10.1038/s41612-022-00296-w

References From the Supporting Information

North, G., Bell, T., Cahalan, R., & Moeng, F. (1982). Sampling errors in the estimation of empirical orthogonal functions. *Monthly Weather Review*, *110*(7), 699–706. https://doi.org/10.1175/1520-0493(1982)110<0699:seiteo>2.0.co;2

Plumb, R. A. (1985). On the three-dimensional propagation of stationary waves. *Journal of the Atmospheric Sciences*, *42*(3), 217–229. https://doi.org/10.1175/1520-0469(1985)042<0217:ottdpo>2.0.co;2